GTI ENERGY
solutions that transform

NON-CONFIDENTIAL FINAL REPORT

OTD PROJECT NUMBER: 7.22.j

Evaluation of Current Advanced Mobile Leak Detection Systems

Public Report Issued:

January 2026

GTI Energy Contact:

Christopher Moore, PhD
cmoore@gti.energy

1700 S. Mount Prospect Rd.
Des Plaines, Illinois 60018

www.gti.energy

LEGAL NOTICE

This information was prepared by GTI Energy for Operations Technology Development under 7.22.j. Neither GTI Energy, the members of GTI Energy, any GTI Energy sponsor(s) or customer(s), nor any person acting on behalf of any of them:

a) Makes any warranty or representation, express or implied with respect to the accuracy, completeness, or usefulness of the information contained in this report, or that the use of any information, apparatus, method, or process disclosed in this report may not infringe privately-owned rights. Inasmuch as this project is experimental in nature, the technical information, results, or conclusions cannot be predicted. Conclusions and analysis of results by GTI Energy represent GTI Energy's opinion based on inferences from measurements, empirical relationships, and/or other data and factual information, which inferences and assumptions are not infallible, and with respect to which competent specialists may differ.

b) Assumes any liability with respect to the use of, or for any and all damages resulting from the use of, any information, apparatus, method, or process disclosed in this report; any other use of, or reliance on, this report by any third party is at the third party's sole risk.

The results within this report relate only to any items specifically evaluated or tested.

Executive Summary

Advanced mobile leak detection (AMLD) technologies have potential advantages over traditional walking surveys by identifying small emissions, sensing leaks farther from the measurement point, increasing efficiency through targeted follow-up, and reducing dependence on operator expertise. However, local distribution companies have reported mixed results. As discussed in stakeholder AMLD user group meetings, while some companies have had good success with AMLD, others have experienced challenges including low and inconsistent leak confirmation rates (e.g., finding gradable leaks)—sometimes as low as 40%—which reduce survey efficiency and raise questions about follow-up procedures, instrument sensitivity, search adequacy, and how indications should be processed. High volumes of indications can also delay investigations. Due to the many possible advantages of AMLD, this project was focused on exploring the root factors that may lead to variations in performance that some companies observe.

The high-sensitivity, methane-specific instruments that have emerged over the last few years have slowly gained acceptance and are now promoted by regulatory bodies, yet only a limited number of studies have been conducted and published.[1][2][3][4] Most studies have been conducted internally within gas companies independently or in collaboration with vendors, often resulting in proprietary data that is not widely available. This presents an opportunity for mixed information and understanding across the industry.

The project's objective was to identify key factors influencing the performance of leading technologies used in AMLD surveys. This project conducted field testing of two highly sensitive pumped systems, representative of typical AMLD approaches. Controlled field testing was conducted in a large open area to establish the relationship between detection rate and vehicle speed, leak rate, and the distance between the measurement and the leak.

Performance was evaluated using the true positive rate, the percent of tests with methane emissions that led to an indication, and the false positive rate, the percent of tests without methane emissions that led to an indication. Both devices were installed on the front of one vehicle to ensure the devices passed through a leak plume under essentially identical conditions. A simple detection algorithm designed by GTI Energy was used for both instruments, and testing also investigated the threshold used to define a leak indication. As such, these results may differ from those calculated using the proprietary software often offered by AMLD vendors.

We found that vehicle speeds above 20 mph, a distance from the leak source of 60 feet, and leak rates of 5 scfh or lower led to declines in true positive rates. Smaller leaks are detectable with AMLD instruments, but other factors need to be favorable (i.e., close to leak source and low vehicle speed). The leak rate and the detection threshold had the most pronounced effect on the true positive and false positive rates across the range of conditions tested.

Under ideal conditions, as presented in this study, the true positive rate is reasonably good (in the range of 80 to 90%), but the false positive rate increases for detection thresholds below 0.05 ppm. A slightly higher threshold would reduce the false positive rate, but detection rates rapidly decrease below 80%. As real-world environments include additional variables not captured in this study, further testing in representative settings may provide additional insights into AMLD performance, particularly in complex urban environments.

Contents

Executive Summary 3
Contents 4
Figures 5
Tables 6
Abbreviations and Acronyms 7
Introduction 8
Project Objective 8
Background 8
Business Value 8
Field Testing 9
Results 11
Data Processing 11
Statistical Analysis Approach 15
Data Analysis 16
True Positive Rate (TPR) 16
False Positive Rate (FPR) 16
Discussion 18
Instrumentation influence on TPR 18
Wind influence on TPR 18
Speed influence on TPR 19
Distance influence on TPR 21
Leak Rate influence on TPR 21
Position of instruments 23
Combined influence factors 23
Comparison with Previous Study 23
Observations of Interest: 24
Plume elongation due to vehicle passing through it 24
Infrastructure impacts on detection 24
Limits of detectability 25
Conclusions 27
References 28

Figures

Figure 1: Aerial view of parking lot used for field testing and locations of generated leaks.. 9
Figure 2: Setup of generated leak during controlled field testing.. 10
Figure 3: Detection processing flow for the GTI Energy algorithm 12
Figure 4: Example of raw data collected using one of the systems.....13
Figure 5: Example of post-detection location data from one of the systems 14
Figure 6: Example of post-processed data using one of the systems 15
Figure 7: Overall True Positive Rate (TPR) results for testing in open-field conditions 16
Figure 8: Overall False Positive Rate (FPR) results for testing in open field conditions 17
Figure 9: Wind conditions were mild during controlled testing with no strong winds 19
Figure 10: TPR per driving speed for all leak rates and distances 20
Figure 11: TPR per distance from the source for all leak rates and driving speeds 21
Figure 12: TPR per leak rate for all driving speeds and distances from the source 22
Figure 13: Best- and worst-case TPR conditions.....23
Figure 14: Location of a leak behind a building 25
Figure 15: The vehicle drove in a zig-zag pattern downwind from the source to observe the possible detection distance. 26

Tables

Table 1. 15

Abbreviations and Acronyms

AMLD ..... Advanced Mobile Leak Detection

AUC ..... Area Under the Curve

FPR ..... False Positive Rate

GPS ..... Global Positioning System

OTD ..... Operations Technology Development

PHMSA ..... Pipeline and Hazardous Materials Safety Administration

PIPES ..... Protecting Our Infrastructure of Pipelines and Enhancing Safety

RMLD-CS ..... Remote Methane Leak Detector-Complete Solution® Heath Consultants, Inc.

ROC ..... Receiver Operating Characteristic

TIC ..... Unitless time constant (typically the sample rate)

TPR ..... True Positive Rate

Introduction

Project Objective

This project evaluated the leak detection performance and quantification capabilities of two commercially available advanced mobile leak detection (AMLD) systems and identified key factors influencing their performance. Controlled field testing was conducted with two highly sensitive pumped systems representative of typical AMLD approaches to determine factors impacting the technology's performance. The study conducted extensive controlled testing to determine the effects of vehicle speed, leak rate, distance of measurement to leak, and wind speed on leak detection performance. This evaluation improved the understanding of AMLD limitations and aided in determining the suitability of these technologies to meet operator needs.

Background

The Protecting Our Infrastructure of Pipelines and Enhancing Safety Act of 2020 (PIPES Act) emphasized the use of advanced leak detection technologies in leak surveys, and specifically mentioned equipment mounted on mobile platforms. Commercially available AMLD systems which improve upon the sensitivity limitations of traditional mobile leak survey methods have since entered the market.

A completed PHMSA/OTD funded GTI Energy project – Validation of Remote Sensing and Leak Detection Technologies under Realistic and Differing Conditions (PHMSA Project #693JK31910006POTA/OTD Project 7.20.b) – provides the framework for evaluating advanced leak detection technologies used in this project and streamlined the data collection planning process. The framework includes techniques for balancing tradeoffs between true positives (correct detections), false positives (detecting leaks when no leak is present), true negatives (detecting no leak when no leak is present), and false negatives (missing leaks). These techniques examine probability of detection statistics coupled with receiver operating characteristic (ROC) curves and area under the curve (AUC) statistics.

Business Value

The PIPES Act requires all pipeline operators to adopt advanced leak detection technologies and practices to detect pipeline leaks. Studies that clearly outline methods to understand and improve performance can support rapid adoption and effective implementation. The AMLD platform has grown to include several commercial products, and it has become crucial to evaluate their performance and determine use cases for these systems (i.e., regulatory leak survey or supplemental leak identification).

Field Testing

Controlled field testing was conducted at an empty, open parking lot in October and November 2023. The devices were installed on a single utility-owned vehicle the week of October 16th and field tested the week of October 30th.

Controlled testing was conducted in a parking lot, simulating performance in a large, open area. **Figure 1** provides an aerial view of the leak locations at this parking lot. This type of location was chosen to minimize wind instability and provided clean plumes blowing downwind to drive through. Five passes were conducted for each of the 65 individual controlled tests, and included varying leak rates (0, 0.5, 1, 5, 10, and 20 scfh), distance from the leak (10, 30, and 60 feet), and speed of the vehicle (5, 10, 20, and 30 mph). Each of these 5 passes was treated as an independent experiment with a single "detect" or "no detect" result. Results across these 5 passes were used to calculate detection statistics for the given set of conditions. These experiments did not consider results as a function of the number of passes. An anemometer was also placed on site to measure the wind speed and direction. **Figure 2** illustrates the setup for the controlled testing in a large open area, where the vehicle drove downwind of the generated leaks. Blank leaks (no flow) were also used to collect false positive data.

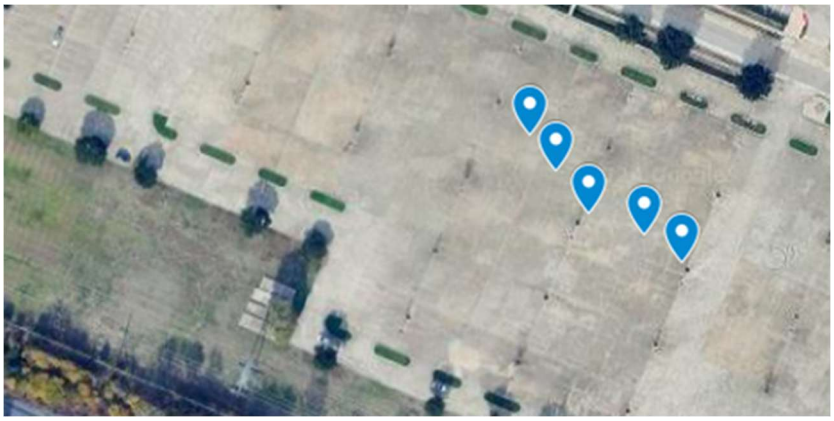


Figure 1: Aerial view of parking lot used for field testing and locations of generated leaks. The location of the leak source was periodically changed to ensure that the vehicle had a safe path to drive and maintain driving downwind from the source.

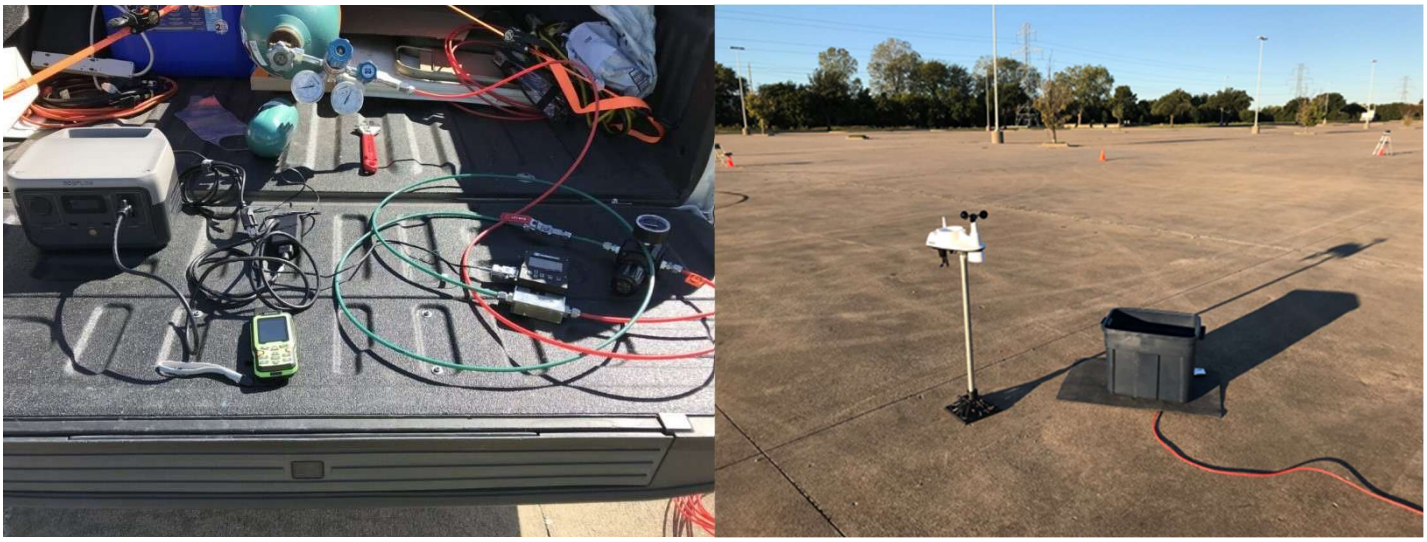


Figure 2: Setup of generated leak during controlled field testing. The equipment is set up in the back of a vehicle (left). A mass flow controller is connected to a gas cylinder to generate a gas leak (right). The tubing is placed under a rug to slow the speed of the flow, and the vehicle path was then marked to ensure a consistent path of the vehicle downwind from the leak source. Wind speed and direction was measured at the leak location.

Results

Data files created by the two AMLD systems were first organized by leak, then data was extracted and analyzed using MATLAB programming. The instruments' data character varied and therefore the data extraction process was slightly different for each device.

Data Processing

Specific MATLAB scripts were created to import, process, and present raw data log files from AMLD instruments as outlined in **Figure 3**. Initial raw data was plotted to verify data collection as shown in **Figure 4**. Data when the vehicle was not moving was then filtered out as shown in the top panels of **Figure 5**. The data was then processed through a simple 20 point moving average filter to generate a methane background estimate. The current reading was then compared to this background and if the difference was greater than a detection threshold it was considered a detection. This was plotted as 0 (no detection) or 1 (detection) as shown in the bottom panels of **Figure 5**. Passes were identified either by time separation or a GPS location test. The detections, visualized as shown in **Figure 6**, were then examined to identify if a detection occurred during a pass, and the number of detections was recorded for each detection threshold considered. The example data in these figures is from a test run conducted at a gas leak training facility nearby.

GTI Energy applied this basic detection algorithm to all instruments. The simple 20 point moving average detection approach was used with varying detection thresholds to allow a sensitivity study of the detection threshold to be conducted. The moving average window size is subjective, based on a compromise between detector response speed and signal variance. The smaller the window, the faster the response at the expense of false detections on noise (i.e., false positives). The larger the window, the slower the response, which will reduce false positives but increase the risk of missing a real detection. The detections were then evaluated if they were within a pass. If so, a True Positive was given. Specific detection thresholds and algorithm implementation by different vendors did not factor into the analysis. The simple peak identification algorithm used by GTI Energy does not consider other factors (such as wind) and may be much simpler than the proprietary algorithms vendors use to indicate leaks. As the goal is to better understand the factors that influence AMLD in general, a consistent simple algorithm applied to multiple AMLD systems was considered sufficient as it enabled an assessment of the change caused by individual factors.

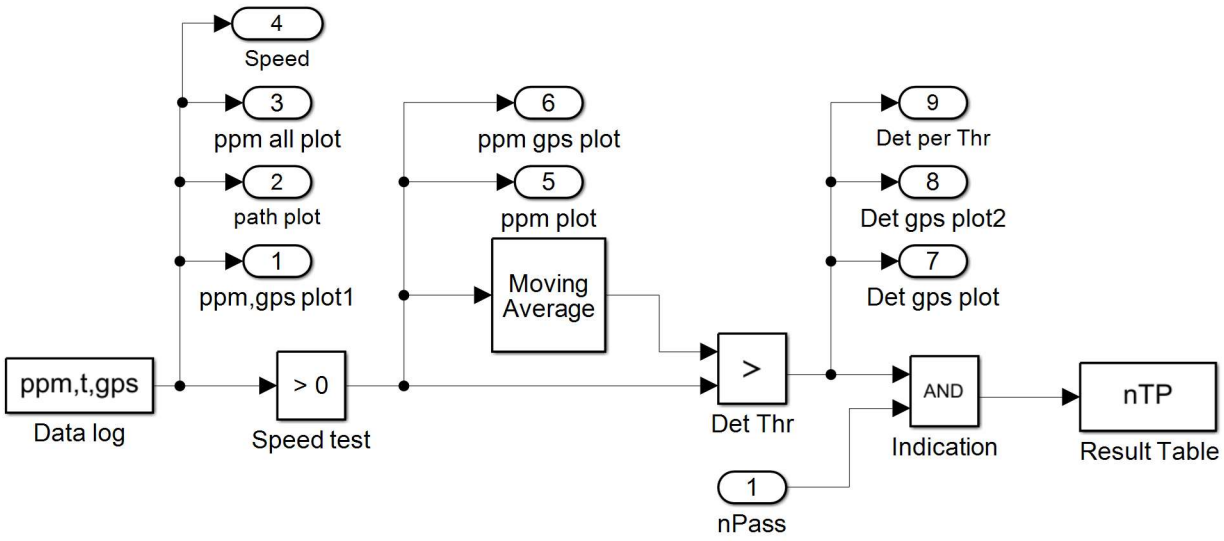


Figure 3: Detection processing flow for the GTI Energy algorithm. A simple 20 point moving average detection approach was used with varying detection thresholds. The detections were then evaluated if they were within a pass. If so, a True Positive was given.

Figure 4 provides an example of the raw data collected using one of the systems. Data collected includes (top left clockwise):

- Peak concentration measurements along a latitude/longitude area
- GPS path taken
- Concentration measurements for the duration of the test
- Speed of the vehicle for the duration of the test

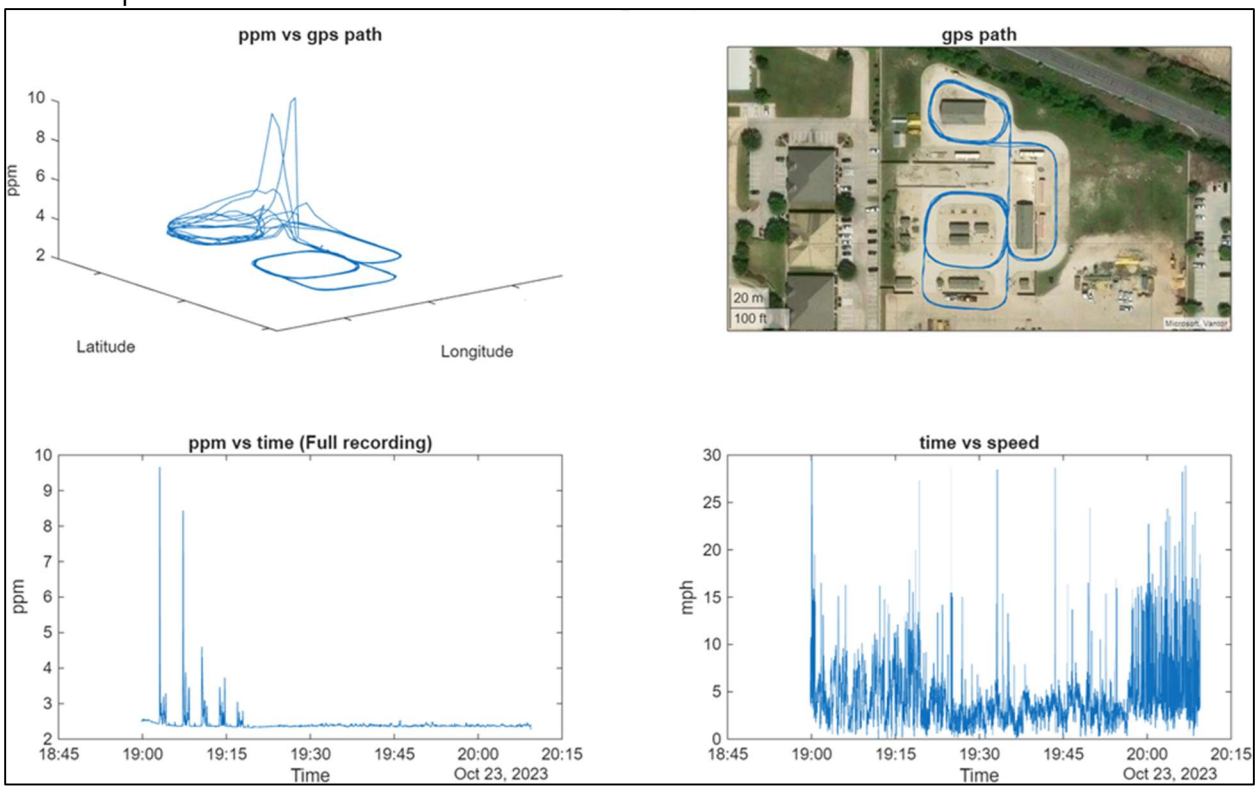


Figure 4: Example of raw data collected using one of the systems.

Figure 5 provides an example of post-detection location data and **Figure 6** shows the post-processed detections for threshold of 0.01, 0.05, 0.1, 0.2, 0.5 and 1.0 ppm. Data processing includes (top left clockwise):

- Ppm data while vehicle in motion
- GPS and ppm data while vehicles are in motion
- Detections vs GPS (detection threshold of .01 ppm shown, top-down view)
- Detections vs GPS (detection threshold of .01 ppm shown)

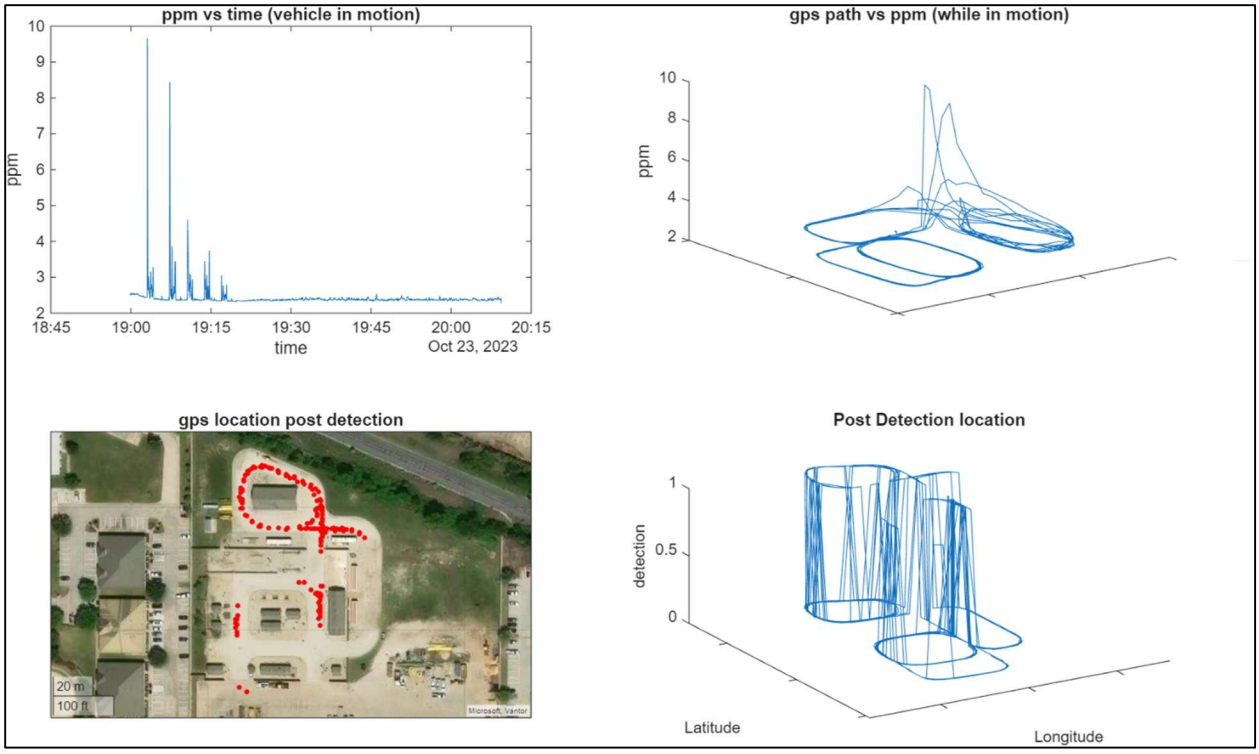


Figure 5: Example of post-detection location data from one of the systems. Data is filtered for when the vehicle is moving, and then detections are calculated using the detection algorithm.

Figure 6 depicts detections plotted as a function of time for the different detection thresholds of .01, .05, .1, .2 .5 and 1 ppm.

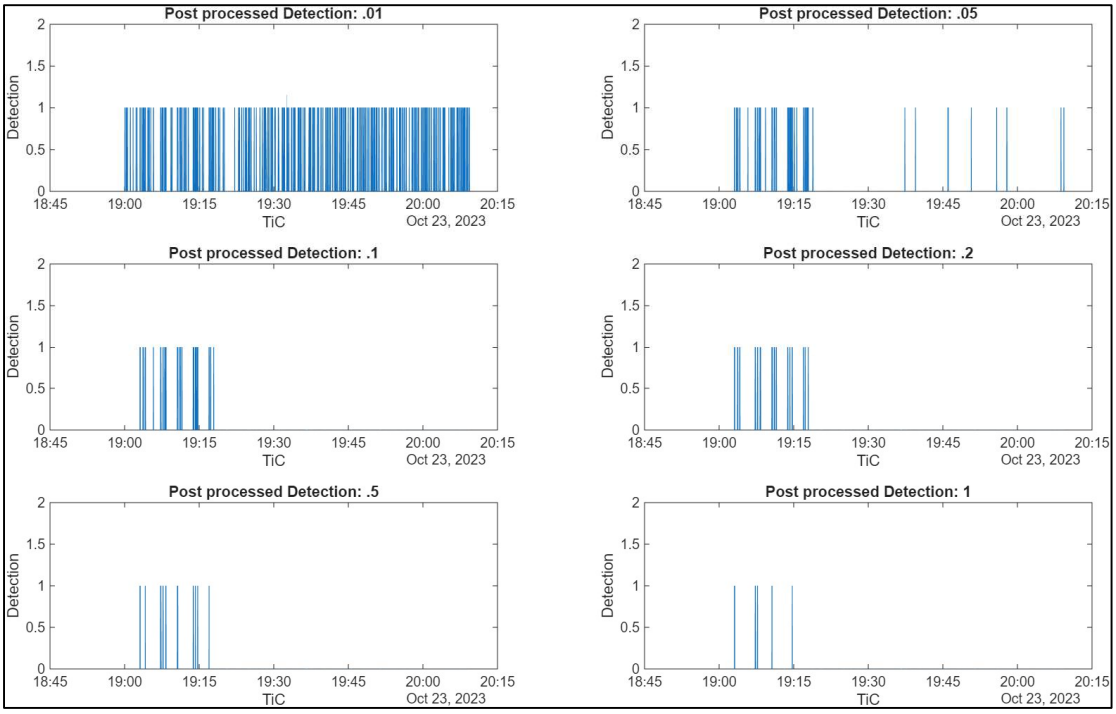


Figure 6: Example of post-processed data using one of the systems. Detections are plotted for each detection threshold. The value of one indicates a detection.

Statistical Analysis Approach

The AMLD performance analysis is based on a confusion matrix as illustrated in **Table 1**. In the presence of a leak, a detection is classified as a True Positive (TP), while no detection (miss) is classified as a False Negative (FN). In the absence of a leak, no detection is classified as a True Negative (TN), and a detection (in the absence of a leak) is classified as a False Positive (FP). These are determined for each pass separately. Performance results across passes for a given set of conditions are then represented by the following formulas:

- True Positive Rate: $TPR = TP/(TP + FN)$
- False Positive Rate: $\mathrm{FPR} = \mathrm{FP}/(TN + FP)$

		Predicted
Actual	# True Positive (TP) (detect)	# False Negative (FN) (miss)
	# False Positive (FP) (false alarm)	# True Negative (TN) (correct no detect)

Table 1: Total detection performance illustrated as a confusion matrix. In the presence of a leak, a detection is classified as a True Positive (TP), while no detection (miss) is classified as a False Negative (FN). In the absence of a leak, no detection is classified as True Negative (TN), and a detection is classified as False Positive (FP).

Data Analysis

True Positive Rate (TPR)

The overall TPR is shown in **Figure 7**. Additional TPR charts are computed for each conditional variable of the study including driving speed, distance from leak, and leak rate. The TPR falls well below the 80% level once the detection threshold rises above 0.2 ppm.

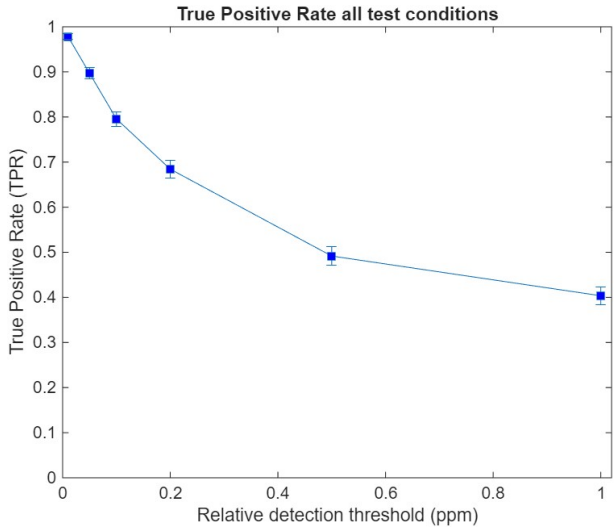


Figure 7: Overall True Positive Rate (TPR) results for testing in open-field conditions. Error bars shown represent the standard error – these represent uncertainty based on sample size and variability across samples. The average results across instruments are shown.

False Positive Rate (FPR)

'Blank' tests with no release of gas were conducted to estimate the FPR. The overall FPR is shown in **Figure 8**. The FPR increases as the detection threshold is reduced below 0.1 ppm, though it remains low.

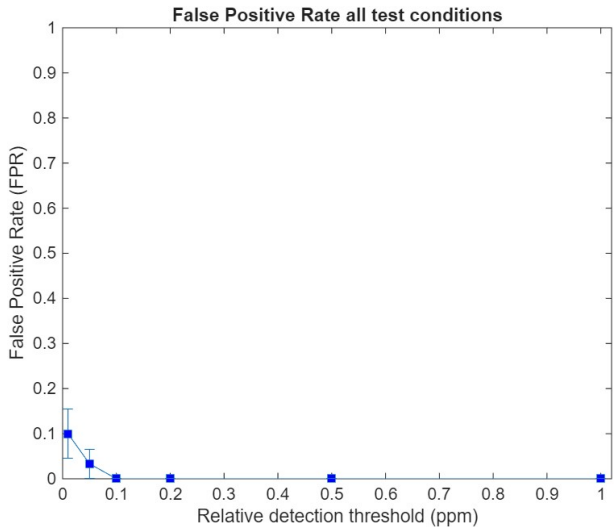


Figure 8: Overall False Positive Rate (FPR) results for testing in open field conditions. FPR results are calculated from tests with no leaks present. False Positives increase below thresholds of 0.1 ppm. Error bars shown represent the standard error – these represent uncertainty based on sample size and variability across samples. The average results across instruments are shown.

Discussion

Instrumentation influence on TPR

In this study, pumped technologies were utilized. Pumped systems rely on air being drawn into a chamber, where the sensor measures the methane concentration. Open path systems rely on the plume passing through the laser light beam. There are tradeoffs for both approaches related to sensitivity, noise, response time, and detection algorithm. Below is a short discussion of these tradeoffs:

- A pumped system will have a slower reaction time due to having to draw in the sample. The amount of delay is determined by the draw pump capacity, tubing length, and sample flow design. Specifications of the instruments are not specifically known, but both used internal pumps and do not tap off an external high flow pump. A partial sample could also result depending on how the plume is intersected and the speed of passing through. The advantage is that higher sensitivity may be achievable, thus needing less sample concentration to make a detection.
- Open path laser systems will have a fast response to methane as the vehicle passes through a plume. The system's sensitivity is typically limited to the total path length of the laser light beam. A longer laser path length increases sensitivity.

Instrument noise is a key contributor to the sensitivity and ultimately the minimum detection threshold achievable.

Wind influence on TPR

Wind is a major factor in leak detection in general and is anticipated to also impact AMLD. AMLD relies on the atmospheric conditions to either hold the plume down or to blow the plume to a point that a vehicle can drive through it. AMLD leak surveys have trended toward nighttime driving when the wind conditions and atmospheric conditions may be more favorable. This study did not evaluate this aspect due to testing constraints. The study was also limited to the variability of wind speeds during the study. To the extent that wind speeds varied, the effect on TPR is illustrated in **Figure 9**. The TPR improved with a moderate increase in the wind speed. With little to no wind, the methane plume will expand in all directions, thus reducing the methane concentration downwind.

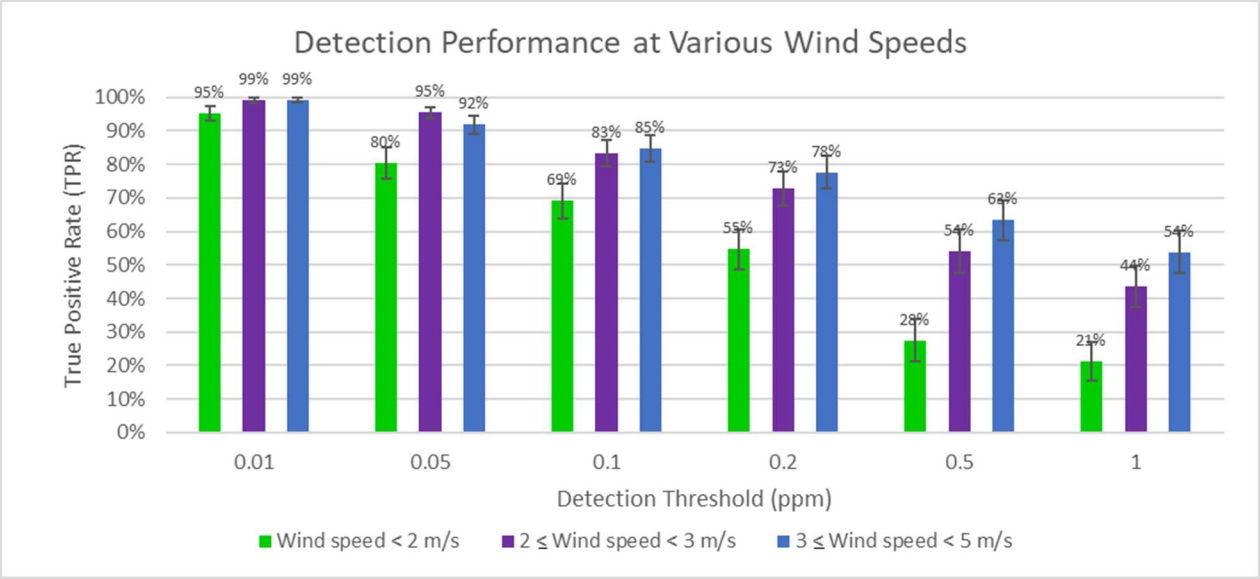


Figure 9: Wind conditions were mild during controlled testing with no strong winds. However, an increase in the true positive rate is observed when there is a moderate amount of wind to move the plume such that the vehicle will drive through it. Error bars shown represent the standard error – these represent uncertainty based on sample size and variability across samples. The average results across instruments are shown.

Speed influence on TPR

Vehicle speed is also a factor that affects the TPR. The faster the vehicle is moving, the shorter the time the instrument is in contact with the plume. In the extreme, the instrument may only have a fraction of time to make a detection determination, for example, passing through the plume faster than the instrument response rate. The overall effect of vehicle speed is illustrated in **Figure 10**. The TPR observably declines at 20 mph, and it is further reduced by 30 mph in the test.

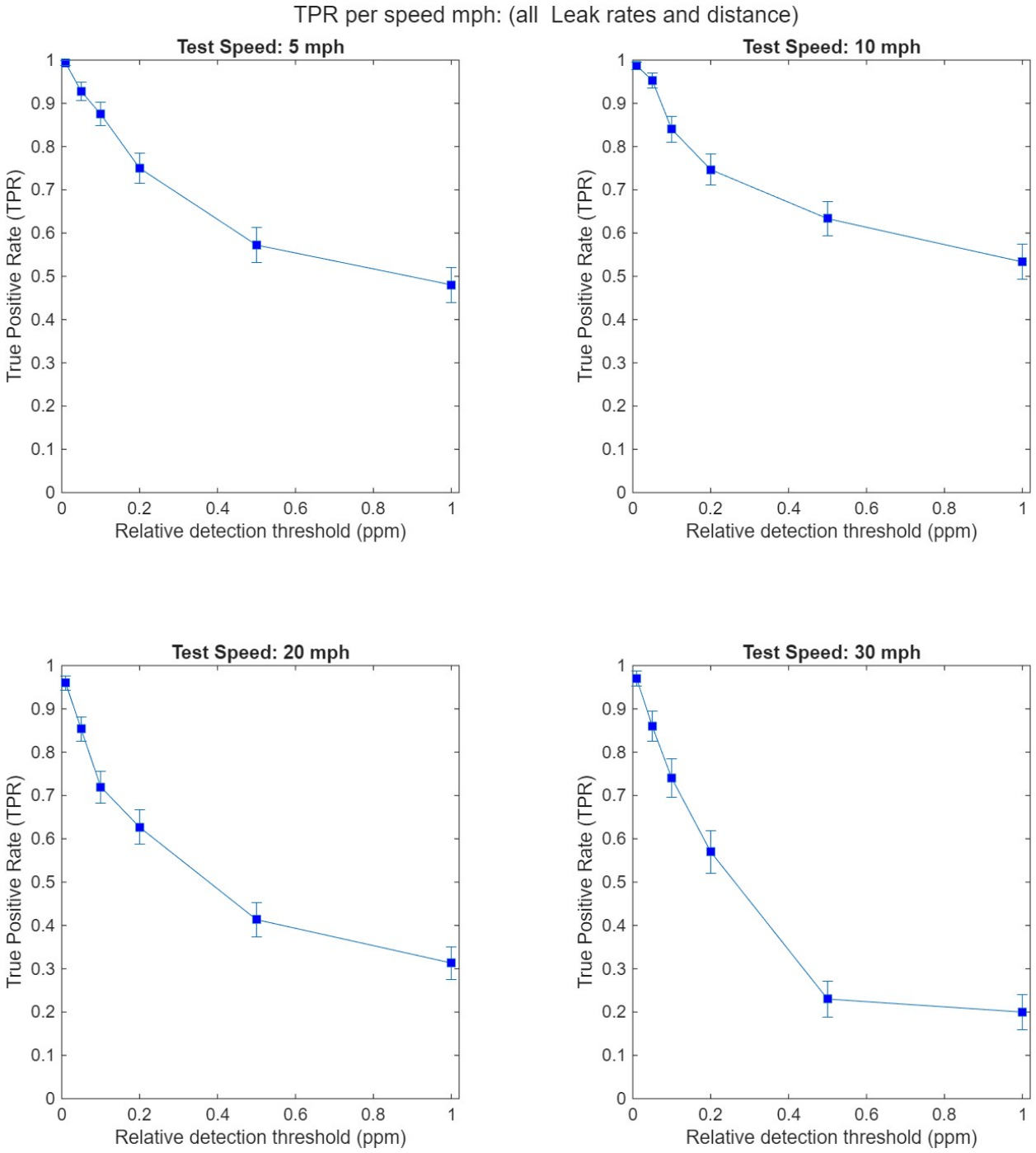


Figure 10: TPR per driving speed for all leak rates and distances. The TPR drops off starting at 20 mph and is lower at 30 mph in the test. Error bars shown represent the standard error – these represent uncertainty based on sample size and variability across samples. The average results across instruments are shown.

Distance influence on TPR

Distance from the source affects the TPR due to the natural concentration dilution as the plume spreads out downwind. Plume dilution is a complex relationship which includes wind speed, surface friction, atmospheric conditions, and distance. This study was conducted in an open field area with minimal ground interference so that a more uniform plume downwind can be expected. The overall effect on the TPR is illustrated in **Figure 11**.

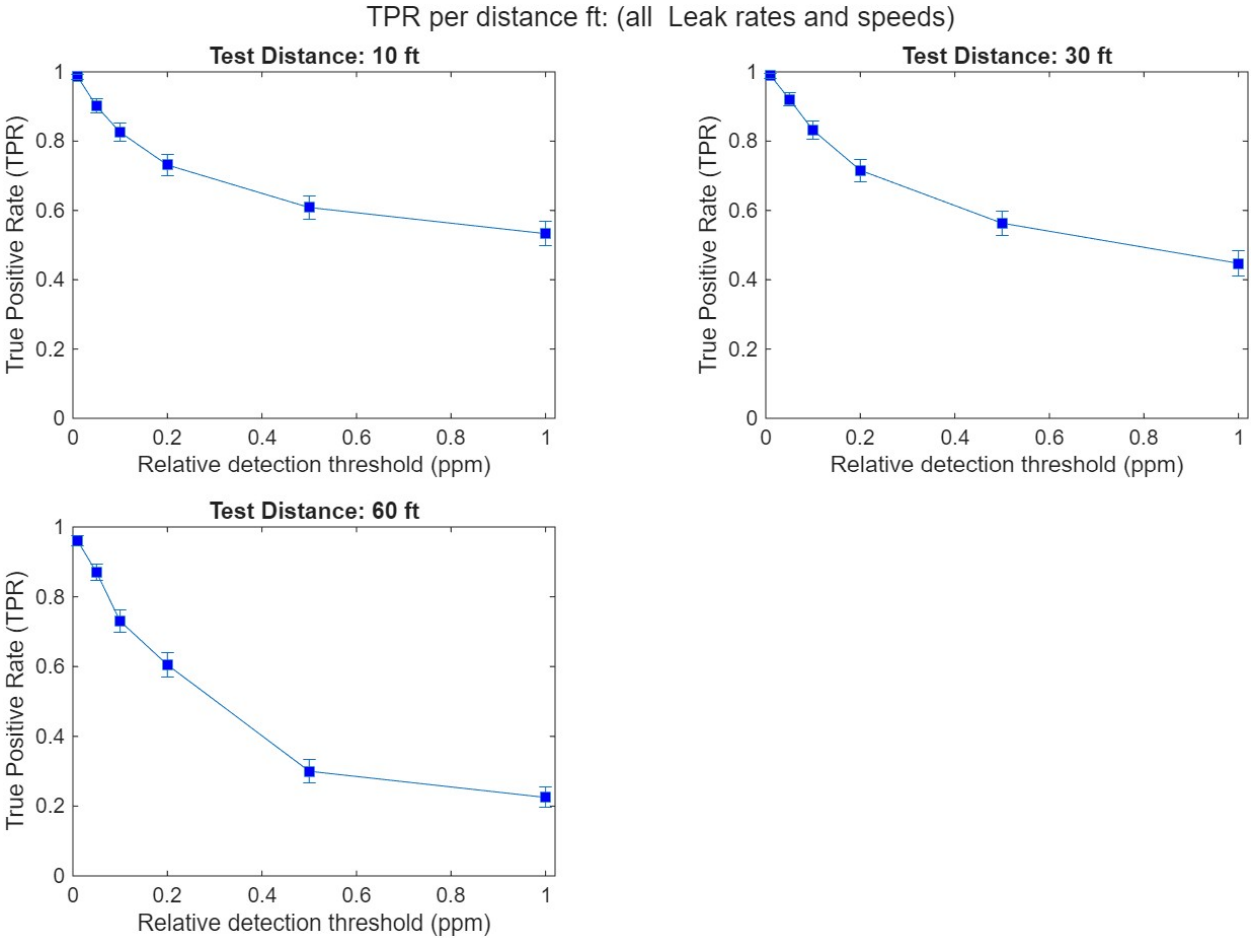


Figure 11: TPR per distance from the source for all leak rates and driving speeds. The TPR slightly decreases as the distance increases. Under ideal conditions, distance from the source may have a lesser impact as the plume holds together better than in conditions with complex plume movement such as in urban environments that have a lot of above ground infrastructure. Error bars shown represent the standard error – these represent uncertainty based on sample size and variability across samples. The average results across instruments are shown.

Leak Rate influence on TPR

The amount of methane emitted plays a role in the detection rate. Actual leaks will emit at different flow rates. This study observes that the TPR reduces with leak rates below 5 scfh. While smaller leak rates are detectable, other factors need to be favorable, such as proximity to the source or the speed of the vehicle. The overall effect of leak rate on the TPR is illustrated in **Figure 12**.

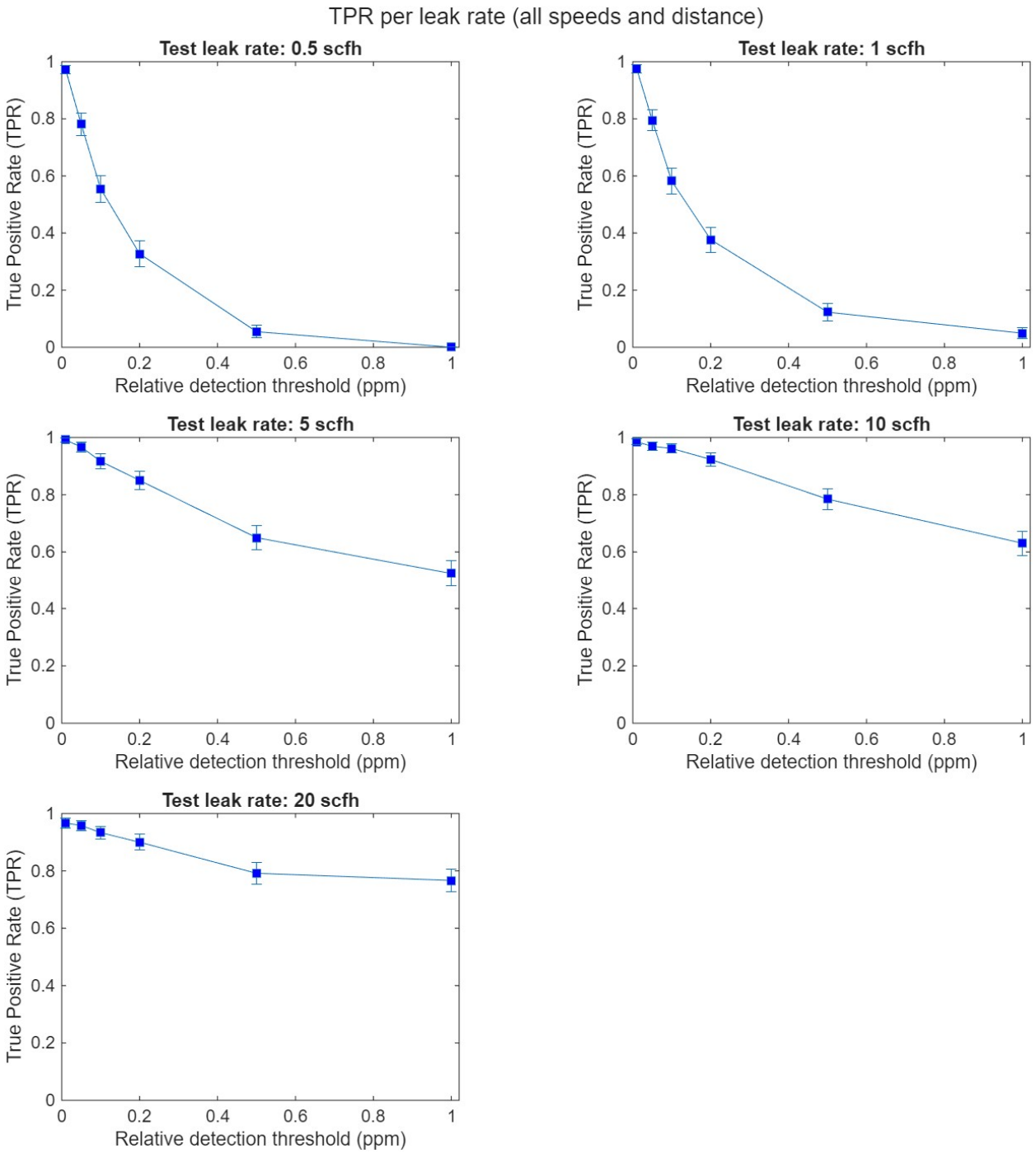


Figure 12: TPR per leak rate for all driving speeds and distances from the source. TPR for low emission rates is very low and does not improve until flow rates increase above 5 scfh. Error bars shown represent the standard error – these represent uncertainty based on sample size and variability across samples. The average results across instruments are shown.

Position of instruments

The height of the instrument sample points was not studied. Instead, it was attempted to have all the instruments at the same level so that all the instruments pass through the same plume path.

Combined influence factors

While the above results attempt to isolate one factor at a time, the actual combinations are much more complex. The TPR can range from very high (close, high flow rate, moderate speed) to very low (far, low flow rate, fast speed). These extremes are illustrated in **Figure 13**.

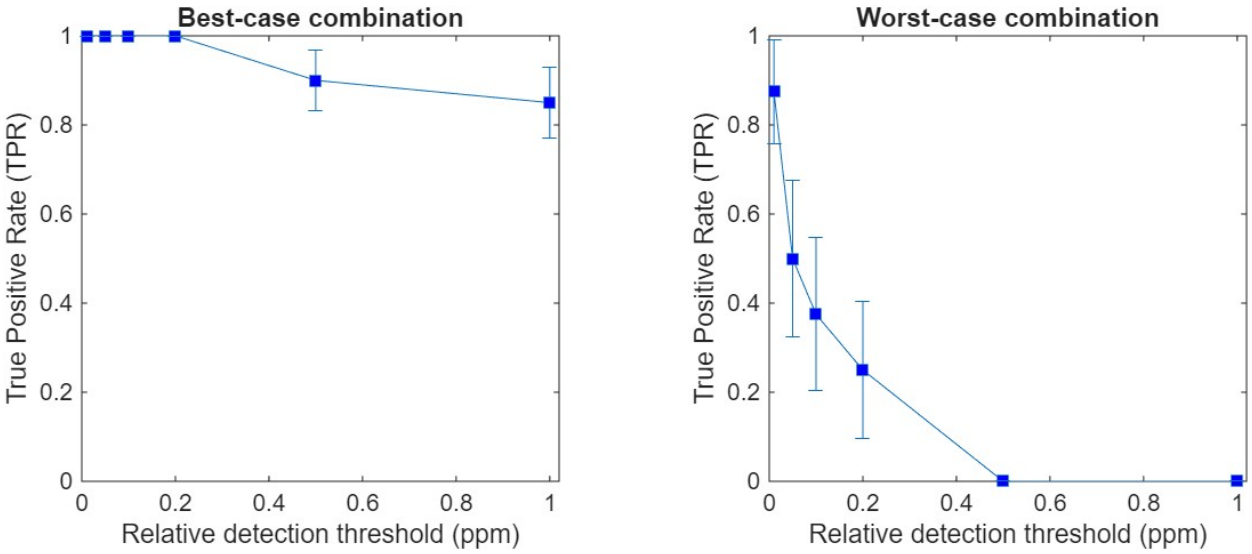


Figure 13: Best- and worst-case TPR conditions. The TPR is high when the leak rate is high (10 scfh), nearby (10 ft), and the vehicle is driving slowly (5 mph) (left). The TPR is low when the leak rate is low (0.5 scfh), far away (60 ft), and the vehicle is driving fast (30 mph) (right). Error bars shown represent the standard error – these represent uncertainty based on sample size and variability across samples. The average results across instruments are shown.

Comparison with Previous Study

Von Fischer, et al (2017) conducted a similar study to determine if leak size could be estimated during a continuous survey by an AMLD system with a limited number of passes (2 to 5) based on methane concentration alone. [3] This project involved 5 separate controlled release experiments at both open and complex sites and used a high-precision methane analyzer from Picarro, GPS system, and a 2-D anemometer. Detected plumes were characterized by the maximum methane concentration, the integrated plume area, and the ratio of the two, respectively. Release rate had a greater impact on these metrics than factors such as vehicle type or any complex factor interactions, with distance having the second largest impact. Notably, variations in wind speed had little to no impact on estimated leak rates in this study.

Observations of Interest:

In addition to the above analyses focused on TPR and FPR, three test runs are of interest and discussed below. Some of these came from additional test runs conducted at a nearby gas leak training facility.

Plume elongation due to vehicle passing through it

It has been observed on several occasions, particularly at higher vehicle speeds, that the gas plume can be pulled/pushed along with the vehicle, resulting in detections even well upwind. These upwind detections were not counted as false positives. Some emission rate quantification calculations factor in the 'plume width'. Consideration should be given by instrument providers to account for this effect. Alternatively, the speed of the vehicle should be limited during an emission rate quantification measurement to reduce this effect. Wind conditions would also play a factor in how much and for how long the plume is stretched. Emission rate quantification was not part of this study; therefore, no measurements were made to validate this observation.

Infrastructure impacts on detection

A particular leak at the gas training facility was located off the road and behind a building (**Figure 14**). The leak was between the back of the building and the facility's brick wall. A strong wind from the south was pushing gas along the wall and then across another wall. Initially, a very small leak (difficult to detect with handheld laser, 48 ppm-m) was flowing. On the next test, the leak was much larger. However, the second test with the higher flow leak was not as detectable. It is assumed that the wind was pushing the plume from the small leak against the wall perpendicular to the wind, causing emissions to "pool" and improving detectability, but slight shifts in wind direction prevented this same phenomenon from occurring with the higher flow leak. This is likely an edge case but demonstrates that infrastructure can sometimes affect the movement of a leak plume in unexpected ways.

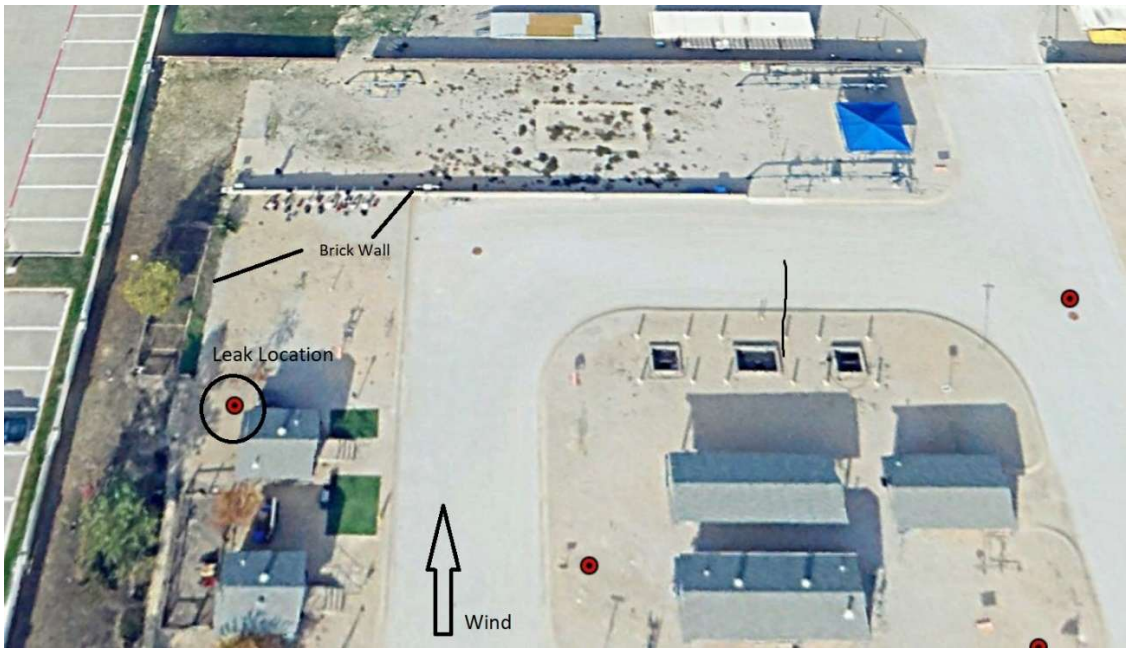


Figure 14: Location of a leak behind a building at the training facility and the brick walls behind and perpendicular to it.

Limits of detectability

After completion of the planned tests, an impromptu test was conducted by driving in a zig-zag pattern downwind of the leak source for as far as the parking lot would allow, to understand the limits of detectability with AMLD. Under the right wind conditions with a slow driving speed, detections were observed for the higher flow rates even when a considerable distance downwind (**Figure 15**). This demonstrates how far one factor can be pushed if other factors are favorable.

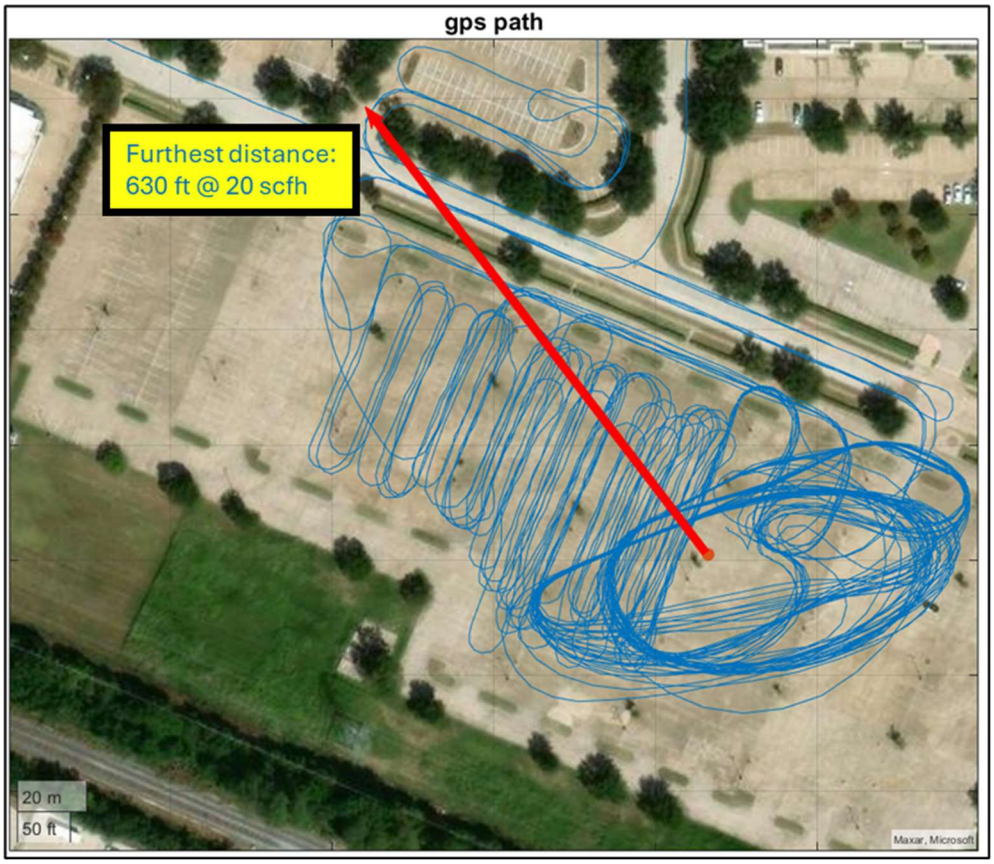


Figure 15: The vehicle drove in a zig-zag pattern downwind from the source to observe the possible detection distance. Under mild wind conditions pushing the plume in a smooth flow, a maximum distance of 630 ft with a flow rate of 20 scfh was observed.

Conclusions

This study focused on evaluating the detection capabilities of two pumped AMLD devices. Controlled release testing was conducted at an open field parking lot to test various factors and their effects on true positive rates (TPR), including leak rate, distance from leak, and vehicle speed. Each of these parameters influenced the TPR demonstrated by the AMLD instruments; however, it is the combination of these factors that drives the TPR and false positive rates (FPR). Higher leak flow rates, a lower distance from the leak source, and a lower vehicle driving speed all contribute to a higher TPR. Alternatively, a worst-case scenario with a low TPR would involve a lower flowing leak, a larger distance from the leak source, and a faster driving speed.

Several challenges were presented throughout the course of this project. During the testing, there were a few operational and logistical challenges faced. Sufficient power was needed when running two instruments on one vehicle and the devices for data collection simultaneously. Weather limitations (heavy rain) were present and paused testing and data collection for a period of time. Collecting and sorting through all the data from the two instruments required time and resources. Each device had a different data output, and therefore required different data analysis scripts to interpret, clean, and compile the data. The data was also collected under different time settings and therefore had to be analyzed and configured in order for the data collected to line up between both devices and be evaluated on the same basis.

When considering each factor in isolation, it was found that the leak flow rate and the detection threshold had the most pronounced effect on the TPR across the range of conditions tested. While smaller leaks are detectable with AMLD instruments, other factors would need to be favorable (i.e., close to leak source and low vehicle speed). There is a balance between not missing leaks and having excessive false positives. This is a key tradeoff that each operator will have to consider. A summary of key findings from these tests includes:

- The higher the flow rate of the leak, the higher the TPR
    - Leak rates of 5 scfh or lower showed declines
- The closer to the leak source, the higher the TPR
    - Distances of 60 feet showed declines
- The longer the contact with the plume (i.e., slower driving speed), the higher the TPR
    - Driving speeds 20 mph and above showed declines

Future investigations may involve further analysis of some of the parameters tested in this study in more realistic urban environments or consider other factors such as wind, vendor algorithm, number of passes used to define a detection, or placement of the instrument on the vehicle. They may also consider the combined impacts across factors, as this work primarily considered each factor independently. This study also did not evaluate emission rate quantification, but rather focused on leak detection capabilities of some AMLD devices, and this can be another avenue to investigate in future work.

References

[1] Luetschwager, E., von Fischer, J. C., & Weller, Z. D. (2021). *Characterizing detection probabilities of advanced mobile leak surveys: Implications for sampling effort and leak size estimation in natural gas distribution systems.* Elementa: Science of the Anthropocene. Retrieved from https://online.ucpress.edu/elementa/article/9/1/00143/117297/Characterizing-detection-probabilities-of-advanced

[2] Ravikumar, A. P., Sreedhara, S., Wang, J., Englander, J., Roda-Stuart, D., Bell, C., . . . Brandt, A. R. (2019). *Single-blind inter-comparison of methane detection technologies – results from the Stanford/EDF Mobile Monitoring Challenge.* Elementa: Science of the Anthropocene. Retrieved from https://online.ucpress.edu/elementa/article/doi/10.1525/elementa.373/112505/Single-blind-inter-comparison-of-methane-detection

[3] von Fischer, J. C., Cooley, D., Chamberlain, S., Gaylord, A., Griebenow, C. J., Hamburg, S. P., . . . Ham, J. (2017). *Rapid, Vehicle-Based Identification of Location and Magnitude of Urban Natural Gas Pipeline Leaks.* American Chemical Society. Retrieved from https://pubs.acs.org/doi/10.1021/acs.est.6b06095

[4] Wehnert, P., & Six, E. (2024). *Discover Advanced Mobile Leak Detection (AMLD) - Natural Gas Leak Surveys Utilitzing Mid-IR Open Path TDLAS.* European Geosciences Union General Assembly 2024 (EGU24). Retrieved from https://meetingorganizer.copernicus.org/EGU24/EGU24-1698.html

[5] IOGP, IPIECA, OGCI. (2023). Recommended practices for methane emissions detection and quantification technologies - upstream. Retrieved from https://www.ogci.com/wp-content/uploads/2023/10/661.pdf